

Probing nuclear bubble structure via neutron star asteroseismology

Hajime Sotani¹*, Kei Iida², and Kazuhiro Oyamatsu³

¹*Division of Theoretical Astronomy, National Astronomical Observatory of Japan, 2-21-1 Osawa, Mitaka, Tokyo 181-8588, Japan*

²*Department of Natural Science, Kochi University, 2-5-1 Akebono-cho, Kochi 780-8520, Japan*

³*Department of Human Informatics, Aichi Shukutoku University, 2-9 Katahira, Nagakute, Aichi 480-1197, Japan*

13 November 2018

ABSTRACT

We consider torsional oscillations that are trapped in a layer of spherical-hole (bubble) nuclear structure, which is expected to occur in the deepest region of the inner crust of a neutron star. Because this layer intervenes between the phase of slab nuclei and the outer core of uniform nuclear matter, torsional oscillations in the bubble phase can be excited separately from usual crustal torsional oscillations. We find from eigenmode analyses for various models of the equation of state of uniform nuclear matter that the fundamental frequencies of such oscillations are almost independent of the incompressibility of symmetric nuclear matter, but strongly depend on the slope parameter of the nuclear symmetry energy L . Although the frequencies are also sensitive to the entrainment effect, i.e., what portion of nucleons outside bubbles contribute to the oscillations, by having such a portion fixed, we can successfully fit the calculated fundamental frequencies of torsional oscillations in the bubble phase inside a star of specific mass and radius as a function of L . By comparing the resultant fitting formula to the frequencies of quasi-periodic oscillations (QPOs) observed from the soft-gamma repeaters, we find that each of the observed low-frequency QPOs can be identified either as a torsional oscillation in the bubble phase or as a usual crustal oscillation, given generally accepted values of L for all the stellar models considered here.

Key words: stars: neutron – equation of state – stars: oscillations

1 INTRODUCTION

Neutron star crusts, which are composed of inhomogeneous neutron-rich nuclear matter embedded in a roughly uniform neutralizing background of electrons, can be unique laboratories to provide us with simultaneous manifestations of superfluids, liquid crystals, and solids. This is because nuclear matter at subnuclear densities and sufficiently low temperatures can exhibit various mixed phases of a liquid composed of protons and neutrons and a neutron gas as a result of the combined effect of the tensor, isoscalar part of the nuclear force and the Coulomb interaction, while keeping both the liquid and the gas in a superfluid state thanks to the central, isovector part of the nuclear force (Pethick & Ravenhall 1995). The crustal region, which is located in the outer part of a neutron star, is observationally more relevant than the inner part, namely, the core region, because of the closer distance to the star’s magnetosphere and surface, from which electromagnetic emission occurs.

From the viewpoint of condensed matter physics, however, the deeper, the more interesting. In fact, roughly spherical nuclei (liquid part), which are predicted to form a body-centered cubic (bcc) lattice at relatively low densities, are considered to fuse into rod-like nuclei in a gas of neutrons when the spherical nuclei become so closely packed as to be almost unstable with respect to quadrupolar deformations. As the density increases further, it is expected that the shape of the liquid part in the crust changes from spherical to cylindrical (rod), slab, cylindrical-hole (tube), and spherical-hole (bubble) structures until matter becomes uniform (Lorenz et al. 1993; Oyamatsu 1993). The rod, slab, tube, and bubble structures are often referred to as nuclear pasta. Since the spherical and bubble phases are solids while the cylindrical, slab, and cylindrical-hole phases are

* E-mail: sotani@yukawa.kyoto-u.ac.jp

liquid crystals, possible observations of global free oscillations from neutron stars could be useful for obtaining information about elastic and superfluid properties of neutron star interiors (Passamonti & Andersson 2012). This technique is known as asteroseismology, which is essentially the same as seismology in the case of the Earth and helioseismology in the case of the Sun. In fact, it has been suggested that the neutron star’s properties such as the mass and radius, the equation of state (EOS) of matter therein, and the magnetic properties would be possible to obtain via the spectra of the star’s oscillations (see, e.g., Van Horn et al. (1995)).

Neutron star asteroseismology is unique in the sense that in addition to electromagnetic waves, gravitational waves radiating from the star are expected to provide us with information about the star’s global oscillations (Andersson & Kokkotas 1996; Sotani, Tominaga & Maeda 2001; Sotani, Kohri & Harada 2004; Sotani et al. 2011; Doneva et al. 2013). Direct gravitational wave detections from neutron stars, which have yet to be done, would be highly promising in the near future.

Meanwhile, there are X-ray observational evidences for neutron star oscillations. In fact, quasi-periodic oscillations (QPOs) were discovered in the X-ray afterglow of giant flares from soft-gamma repeaters (SGRs) (Israel et al. 2005; Strohmayer & Watts 2005, 2006; Huppenkothen et al. 2014), which are supposed to be strongly magnetized neutron stars (Kouveliotou et al. 1998; Hurley et al. 1999). Although there are still many uncertainties in understanding of the mechanism of the giant flares and the subsequent QPOs, it is generally accepted that the QPOs arise from global oscillations of the neutron stars. The observed QPO frequencies are in the range of tens Hz up to kHz, while typical frequencies of neutron star acoustic oscillations are around kHz (Van Horn et al. 1995). Particularly, identification of the QPO frequencies lower than ~ 100 Hz is not straightforward but could significantly constrain the possible origin of the QPOs. Basically, candidates for the corresponding global oscillations are crustal torsional oscillations, magnetic oscillations, and coupled oscillations between these two.

Global magnetic oscillations in neutron stars depend crucially on the magnetic field strength and structure therein (Gabler et al. 2013), but those are still poorly known, particularly in superconducting materials, as well as the EOS for matter in the core. In order to avoid such uncertainties, in this paper we simply consider the observed low-lying QPOs as crustal torsional oscillations. In fact, within such identifications, one can obtain information about the crustal properties by fitting the calculated eigenfrequencies to the observed QPO frequencies (Samuelsson & Andersson 2007; Steiner & Watts 2009; Gearheart et al. 2011; Sotani et al. 2012, 2013a,b; Sotani 2014, 2016; Sotani, Iida & Oyamatsu 2016). Because of the success in accurately reproducing all the QPO frequencies, this kind of approach might well play the role of a canonical model for the low-lying QPOs from SGRs. There is nevertheless a serious caveat: To obtain the shear modulus that is consistent with the QPO frequencies, one requires a significantly large value of the parameter L that characterizes the density dependence of the symmetry energy of nuclear matter, as compared with what various nuclear observables suggest.

So far, several calculations of the eigenfrequencies of crustal torsional oscillations have been done by including the effect of superfluidity, but the effect of the possible existence of the pasta structure has been neglected in most of such calculations; an artificial shear modulus has been at most taken into consideration for the pasta phases (Sotani 2011; Passamonti & Pons 2016). Since the crystalline structure in the bubble phase is presumably the same as that in the low density region composed of spherical nuclei, however, one can likewise calculate the eigenfrequencies of the torsional oscillations in the bubble phase. As we shall see, furthermore, the smectic-A liquid-crystalline properties in the phase with slab-shaped nuclei (Pethick & Potekhin 1998) do not allow torsional shear oscillations to occur in linear analysis, which leads to the conclusion that the torsional oscillations in the bubble phase can be excited separately from those in the low density regime. Bearing this in mind, we search for a better fitting to the observed low-lying QPO frequencies while keeping the value of L reasonable.

In Sec. 2 the equilibrium configuration of a neutron star crust is constructed. Section 3 is devoted to eigenmode analyses of torsional shear oscillations within the bubble phase. The resultant eigenfrequencies are compared with the observed QPO frequencies in Sec. 4. Concluding remarks are given in Sec. 5. We use units in which $c = G = 1$, where c and G denote the speed of light and the gravitational constant, respectively.

2 CRUST IN EQUILIBRIUM

We start with description of the equilibrium configuration of a neutron star crust. In this description, we need the EOS of equilibrated crustal matter. For simplicity, we assume that the temperature of the matter is zero. This is a very good approximation in analyzing the crust’s equilibrium configuration and eigenfrequencies of its torsional oscillations, but is not necessarily so in describing damping of such oscillations, which is beyond the scope of the present analysis.

As discussed in Lattimer (1981), the bulk energy per nucleon of uniform nuclear matter at zero temperature can be generally expanded as a function of baryon number density n_b and neutron excess α :

$$w = w_0 + \frac{K_0}{18n_0^2}(n_b - n_0)^2 + \left[S_0 + \frac{L}{3n_0}(n_b - n_0) \right] \alpha^2. \quad (1)$$

Here w_0 , n_0 , and K_0 denote the saturation energy, saturation density, and incompressibility of symmetric nuclear matter ($\alpha = 0$), while S_0 and L are associated with the density dependent symmetry energy $S(n_b)$, i.e., $S_0 \equiv S(n_0)$ and

$L \equiv 3n_0(dS/dn_b)_{n_b=n_0}$. Since w_0 , n_0 , and S_0 characterize the saturated, nearly symmetric nuclear matter, these three parameters are relatively well constrained from empirical data for masses and radii of stable nuclei as compared to the remaining parameters L and K_0 , which characterize the way the energy changes as the baryon density changes from the saturation point of symmetric nuclear matter. With increasing α , the saturation density n_s and energy w_s changes from n_0 and w_0 as

$$n_s = n_0 - \frac{3n_0L}{K_0}\alpha^2, \quad (2)$$

$$w_s = w_0 + S_0\alpha^2. \quad (3)$$

Two of the authors (Oyamatsu & Iida 2003) have derived a phenomenological model for the EOS of uniform nuclear matter in such a way that the bulk energy of nuclear matter reproduces Eq. (1) in the limit of $n_b \rightarrow n_0$ and $\alpha \rightarrow 0$. Within a simplified version of the extended Thomas-Fermi theory for a nucleus of mass number A , the most relevant values of w_0 , n_0 , and S_0 were obtained by fitting the calculated mass excess, charge radius, and charge number of stable nuclei to the empirical data for given values of $y \equiv -K_0S_0/(3n_0L)$ and K_0 . To obtain the equilibrium nuclear shape and size in neutral matter in the crust, furthermore, Oyamatsu & Iida (2007) have derived the optimal energy density and nucleon distribution as a function of n_b within a Wigner-Seitz approximation by taking into account the presence of a gas of dripped neutrons and a uniform electron gas, as well as the five nuclear shapes (sphere, cylinder, slab, tube, bubble). The EOS parameter sets adopted in this paper are shown in Table 1.

We turn to the equilibrium phase transitions between various nuclear shapes. For description of such phase transitions for various sets of the EOS parameters L and K_0 , as in Oyamatsu & Iida (2007), we obtain the optimal energy densities of the five liquid-gas mixed phases and the homogeneous phase at given baryon density and then identify the phase with minimal energy density, i.e., the equilibrium phase. Note that all the phase transitions considered here are of first order. In a star, where the pressure increases continuously with depth, the baryon density is discontinuous at the transition points. Since such discontinuities are negligibly small, however, we will regard it as continuous in calculating the star's structure.

In Fig. 1, for each EOS parameter set (K_0 , L), we display the resultant baryon density at the phase transitions from spherical to cylindrical nuclei (SP-C), from cylindrical to slablike nuclei (C-S), from slablike to cylindrical-hole nuclei (S-CH), from cylindrical-hole to spherical-hole (bubble) nuclei (CH-SH), and from spherical-hole nuclei to uniform matter (SH-U), respectively. In this figure (left panel), the L dependence of the transition densities is remarkable in the sense that all the transition densities seemingly converge to $\sim 0.07 \text{ fm}^{-3}$ with increment in L . This is because a larger L , or, equivalently, a smaller symmetry energy at subnuclear densities, acts to decrease the density of a liquid part (see Eq. (2)) and simultaneously increase the density of a gas of dripped neutrons, as can be clearly seen in Fig. 6 of Oyamatsu & Iida (2007). Moreover, the K_0 dependence of the transition densities is implicit in the fluctuating pattern of each transition line: The larger K_0 , the larger transition density. Instead of these transition baryon densities, we plot, in right panel, $(n_0n_b)^{1/2}$ where we set n_b to the transition densities. Apparently, $(n_0n_b)^{1/2}$ has only a weak dependence on K_0 . This is because the tendency that n_0 decreases with increasing K_0 , which comes mainly from the fitting to empirical charge radii of stable nuclei (Oyamatsu & Iida 2003), plays a role in counteracting the K_0 dependence of the transition densities. Incidentally, the latter dependence stems partly from the conclusion of a liquid-drop model (Oyamatsu, Hashimoto & Yamada 1984) that each shape transition occurs when the volume fraction of a liquid part reaches a critical constant value and partly from the fact that at large neutron excess, K_0 affects the relation between the volume fraction and the baryon density by increasing the density of a liquid part (see Eq. (2)).

Additionally, in Table 1, we list the values of the phase transition density from spherical to cylindrical nuclei, from cylindrical-hole to spherical-hole nuclei, and from spherical-hole nuclei to uniform matter. We remark that all the pasta structures are predicted to appear for all the EOS parameter sets shown in this table except the cases of $(K_0, L) = (360, 76.4)$ and $(360, 146.1)$ in MeV. In practice, no pasta structures appear for the case of $(K_0, L) = (360, 146.1)$, i.e., spherical nuclei transform directly to uniform matter at $n_b = 0.06680 \text{ fm}^{-3}$, while only the bubble structure is absent for $(K_0, L) = (360, 76.4)$, i.e., cylindrical-hole nuclei transform to uniform matter at $n_b = 0.07918 \text{ fm}^{-3}$. Thus, the maximum value of L for the bubble structure to appear in neutron stars is predicted to be $L \simeq 75 \text{ MeV}$.¹ Since we focus on torsional oscillations confined in the bubble phase in this work, we shall consider only the cases with $L \lesssim 75 \text{ MeV}$.

The equilibrium configuration of the crust of a spherically symmetric neutron star is constructed by integrating the Tolman-Oppenheimer-Volkoff (TOV) equations inward from the star's surface down to the crust-core boundary in combination with the crust EOS (Iida & Sato 1997), in such a way that we do not have to use the core EOS, which is uncertain, explicitly. We remark that the crust-core boundary is set to the position where the phase transition occurs from spherical-hole nuclei into uniform matter in the present analysis, while, in the previous studies (Sotani et al. 2012, 2013a,b; Sotani, Iida & Oyamatsu 2016; Sotani 2016), being simply set to the position where the phase transition occurs from spherical nuclei into cylindrical

¹ The maximum value of L for any pasta structures to appear, which is of order 100 MeV, has already been discussed in Oyamatsu & Iida (2007) in terms of fission-like instability of spherical nuclei as well as proton clustering instability in uniform nuclear matter at subnuclear densities.

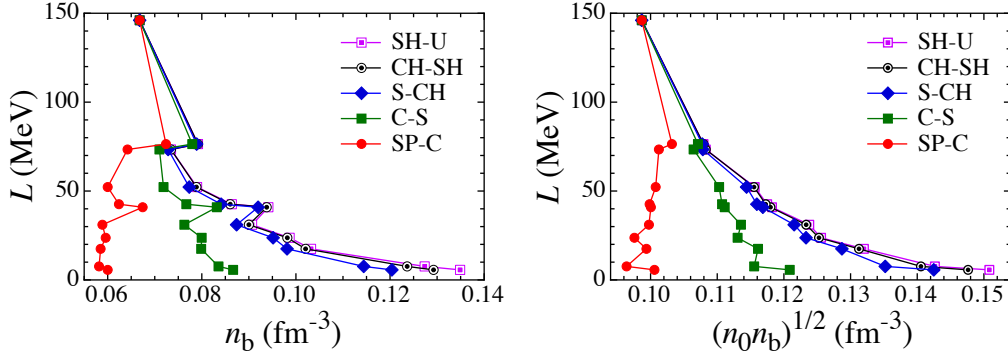


Figure 1. (Color online) The baryon number density n_b (left) and its combination with n_0 , $(n_0 n_b)^{1/2}$ (right), at the structural phase transitions, as plotted for eleven EOS models which are classified by the value of L . Here, the circles, squares, diamonds, double circles, and double squares represent the transition densities from spherical to cylindrical nuclei (SP-C), from cylindrical to slablike nuclei (C-S), from slablike to cylindrical-hole nuclei (S-CH), from cylindrical-hole to spherical-hole (bubble) nuclei (CH-SH), and from spherical-hole nuclei to uniform matter (SH-U), respectively. The data are extracted from Oyamatsu & Iida (2007).

Table 1. The SP-C, CH-SH, and SH-U transition densities obtained for each EOS model, which is characterized by K_0 and L . The asterisk at the value of K_0 denotes the EOS model by which the spherical-hole phase is not predicted to appear. In this case, the SH-U transition density should read the density at which the system melts into uniform matter.

K_0 (MeV)	L (MeV)	SP-C (fm^{-3})	CH-SH (fm^{-3})	SH-U (fm^{-3})
180	5.7	0.06000	0.12925	0.13489
180	17.5	0.05849	0.10206	0.10321
180	31.0	0.05887	0.09000	0.09068
180	52.2	0.06000	0.07885	0.07899
230	7.6	0.05816	0.12364	0.12736
230	23.7	0.05957	0.09817	0.09866
230	42.6	0.06238	0.08604	0.08637
230	73.4	0.06421	0.07344	0.07345
360	40.9	0.06743	0.09379	0.09414
*360	76.4	0.07239	—	0.07918
*360	146.1	0.06680	—	0.06680

nuclei or uniform matter, depending on whether or not the phase with cylindrical nuclei can be energetically favorable. Under spherical symmetry, the metric can be obtained in terms of the spherical polar coordinates r , θ , and ϕ as

$$ds^2 = -e^{2\Phi} dt^2 + e^{2\Lambda} dr^2 + r^2 d\theta^2 + r^2 \sin^2 \theta d\phi^2, \quad (4)$$

where Φ and Λ are the metric functions that depend only on r . The mass function $m(r)$ is associated with Λ via $\exp(-2\Lambda) = 1 - 2m/r$.

According to the solutions to the TOV equations, the thickness of the bubble phase for typical neutron star models with mass M and radius R depends sensitively on L and is at most ~ 10 m. In Fig. 2, the thickness of the bubble phase is shown for the stellar models with $M = 1.4M_\odot$, $1.8M_\odot$ and $R = 10, 12, 14$ km. We remark that the spherical layer of bubbles is located only within 1.5 km from the star's surface for all the stellar models considered here. It is not the thickness but the radius of this layer that is essential to the fundamental frequencies of torsional oscillations trapped therein. The overtone frequencies are sensitive to the thickness, but are high enough to be beyond the scope of this paper.

The shear modulus of crustal matter is one of the most important properties in describing crustal torsional oscillations. For example, the shear modulus of a bcc lattice of spherical nuclei has been calculated as a function of the charge number Z , the number density of nuclei n_i , and the Wigner-Seitz radius a as (Ogata & Ichimaru 1990; Strohmayer et al. 1991)

$$\mu = 0.1194 \frac{n_i (Ze)^2}{a}, \quad (5)$$

by assuming that each nucleus is a point particle. Although modifications of the shear modulus by electron screening and polycrystalline nature have also been considered by Kobayakov & Pethick (2013, 2015), we adopt the traditional formula for the shear modulus [Eq. (5)] for simplicity in the present analysis. Since the crystalline structure in the bubble phase is presumably

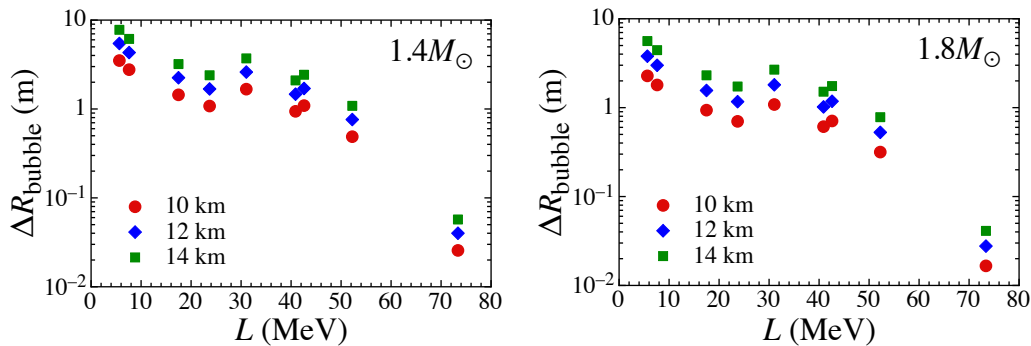


Figure 2. (Color online) Thickness of the bubble phase in the crust of a neutron star. The left and right panels correspond to the cases of $M = 1.4M_{\odot}$ and $1.8M_{\odot}$, respectively, while the circles, diamonds, and squares denote the cases of $R = 10, 12,$ and 14 km.

the same as that in the phase composed of spherical nuclei, we will consider torsional oscillations in the bubble phase by using the shear modulus given by Eq. (5) with appropriate replacements. For the bubble phase, we reinterpret n_i as the number density of bubbles and, as in Watanabe & Iida (2003), replace Z with the effective charge number Z_{bubble} of a bubble. Here, the effective charge number is given by $Z_{\text{bubble}} = n_Q V_{\text{bubble}}$, where V_{bubble} denotes the volume of the bubble, and n_Q is the effective charge number density inside the bubble. n_Q can be calculated as $n_Q = -n_e - (n_p - n_e) = -n_p$ with the number density of protons outside the bubble, n_p , and the number density of a uniform electron gas, n_e , because, in the bubble phase, the background (outside the bubble) charge number density is $n_p - n_e$, while the charge number density inside the bubble is $-n_e$.

The elastic properties in the pasta phases of cylindrical and slab nuclei have also been discussed in terms of liquid crystals (Pethick & Potekhin 1998). In fact, these phases can be regarded as a columnar phase and a smectic A, respectively. For these liquid crystals, the elastic properties and the propagating modes are well known (Landau & Lifshitz 1986; de Gennes & Prost 1993). Pethick & Potekhin (1998) utilized an incompressible liquid-drop model for pasta nuclei to derive the relation between the elastic constants involved and the Coulomb energy density. We remark that the elastic properties in the cylindrical-hole phase is essentially the same as that in the cylindrical phase. The important aspect of global torsional oscillations in the crust is that a restoring force due to the shear stress is responsible for the propagation of the oscillations. To linear order in displacements of the pasta nuclei, there is no such restoring force in the slab phase,² while nonzero shear modulus in the cylindrical-hole phase plays a role in propagation of a torsional shear wave, often referred to as a “third sound.” Thus, the torsional oscillations that are excited within the cylindrical-hole and bubble phases are expected to be separable from those within the spherical and cylindrical phases, although there could be nonlinear coupling between these two. For simplicity, in the next section, we will consider the torsional oscillations that propagate only in the bubble phase; a “third sound” in the cylindrical hole phase and its connection with the torsional oscillations in the bubble and cylindrical phases will be allowed for elsewhere.

3 BUBBLE TORSIONAL OSCILLATIONS

Let us now calculate the eigenfrequencies of torsional oscillations in the bubble phase that is embedded in the spherically symmetric equilibrium configuration of a neutron star crust as constructed in the previous section. We start with the case in which all the matter components participate in the the oscillations. Since torsional oscillations are incompressible, i.e., the oscillations do not involve the density variation, one can determine their frequencies with high accuracy even within the relativistic Cowling approximation in which the metric is fixed during the oscillations. The perturbation equation that governs the torsional oscillations can be derived from the linearized equation of motion as (Schumaker & Thorne 1983)

$$\mathcal{Y}'' + \left[\left(\frac{4}{r} + \Phi' - \Lambda' \right) + \frac{\mu'}{\mu} \right] \mathcal{Y}' + \left[\frac{H}{\mu} \omega^2 e^{-2\Phi} - \frac{(\ell + 2)(\ell - 1)}{r^2} \right] e^{2\Lambda} \mathcal{Y} = 0, \quad (6)$$

where \mathcal{Y} denotes the Lagrangian displacement in the ϕ direction, H is the enthalpy density defined as $H \equiv p + \varepsilon$ with the pressure p and energy density ε , and ℓ is the angular index. \mathcal{Y} is associated with the ϕ component of the perturbed four

² Even in the incompressible limit, there is a propagating transverse mode, often referred to as a “second sound” (Landau & Lifshitz 1986; de Gennes & Prost 1993). This mode involves spatially varying interlayer compression, which in turn couples with spatially varying fluid pressure. A similar kind of “second sound” wave can occur in the columnar phase. All of these modes are beyond the scope of the present analysis.

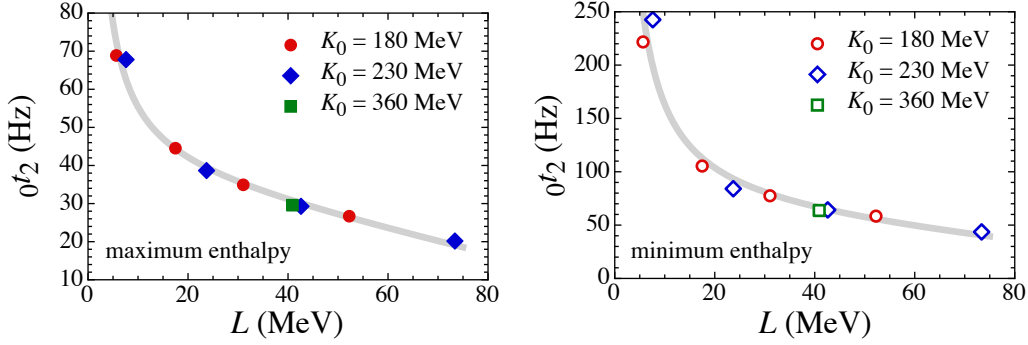


Figure 3. (Color online) Eigenfrequencies of the $\ell = 2$ fundamental torsional oscillations in the bubble phase, calculated for the stellar models with $M = 1.4M_{\odot}$ and $R = 12$ km, as well as with various combinations of K_0 and L . The circles, diamonds, and squares denote the frequencies obtained for $K_0 = 180, 230,$ and 360 MeV, respectively. The left panel corresponds to the numerical results in the case in which all the constituents contribute to the oscillations, while the right panel, in the case in which only the dripped neutrons inside a bubble contribute to the oscillations. In both panels, the thick solid lines denote the fitting given by Eq. (7).

velocity as $\delta u^{\phi} = e^{-\Phi} \partial_t \mathcal{Y}(t, r) (\sin \theta)^{-1} \partial_{\theta} P_{\ell}(\cos \theta)$, where $P_{\ell}(\cos \theta)$ is the ℓ -th order Legendre polynomial. As mentioned in the previous section, we assume the situation in which torsional oscillations occur solely in the bubble phase. In terms of the boundary conditions, this situation conforms to the zero-traction conditions, i.e., $\mathcal{Y}' = 0$ at the inner and outer boundaries of the bubble phase.

It is well known that the frequencies of torsional oscillations are proportional to the shear velocity defined as $v_s = (\mu/H)^{1/2}$ (Hansen & Ciolfi 1980). Thus, not only μ , but also the enthalpy density plays a role in determining the frequencies of torsional oscillations. As in the case of spherical nuclei in a neutron superfluid (Sotani et al. 2013a), we here consider the reduction of the enthalpy density by superfluidity of nuclear matter outside the bubbles. If the whole nuclear matter behaves as a superfluid and only a neutron gas inside the bubbles participate in the oscillations, then, the effective enthalpy density \tilde{H} that contributes to the oscillations would be minimal. In a real world, however, a portion of nuclear matter outside the bubbles comove nondissipatively with the bubbles by undergoing Bragg scattering off the bcc lattice of the bubbles. This effect, often denoted by the entrainment effect, was originally considered for a neutron gas dripped out of the spherical nuclei (Chamel 2012), and hence the effective enthalpy density \tilde{H} could be quantitatively estimated from similar band calculations. Instead of performing such calculations, we mainly analyze the two extreme cases in which the effective enthalpy density is maximal, i.e., $\tilde{H} = H$, and minimal, corresponding to the minimum and maximum frequencies of torsional oscillations in the bubble phase. We remark in passing that in the minimal \tilde{H} case, neutrons inside the bubbles are assumed to oscillate without escaping from the bubble surface or inviting neutrons outside the surface to come in.

For the stellar models with $M = 1.4M_{\odot}$ and $R = 12$ km that are constructed from the EOS with various sets of K_0 and L , the $\ell = 2$ fundamental frequencies of torsional oscillations in the bubble phase are calculated for the two extreme cases of the enthalpy mentioned above. The numerical results are shown in Fig. 3, where the left and right panels correspond to the results for the maximal and minimal enthalpy that contributes to the oscillations, respectively. One can observe that the frequencies of torsional oscillations in the bubble phase are almost independent of the values of K_0 , but strongly depend on the value of L . This L dependence arises mainly from the fact that the proton density outside the bubbles and hence Z_{bubble} decreases with L . In fact, the frequencies for the maximal and minimal enthalpies can be well fitted as a function of L via

$$0t_2 = d_2^{(0)}/L + d_2^{(1)} + d_2^{(2)}L, \quad (7)$$

where $d_2^{(0)}$, $d_2^{(1)}$, and $d_2^{(2)}$ are the adjustable parameters. The resultant fitting lines are also shown in Fig. 3 for $L \leq 75$ MeV. We remark that the fundamental frequencies of torsional oscillations in the crustal region composed of spherical nuclei can also be well fitted as a function of L , but the functional form is different from Eq. (7) (Sotani et al. 2012, 2013a). We also remark that in the case of the minimal enthalpy (no entrainment), the eigenfrequencies in the bubble phase are higher than those in the phase of spherical nuclei by a factor that increases with decreasing L . This is mainly because the gas density is smaller than the liquid density, while decreasing with decreasing L .

4 COMPARISON WITH THE QPO FREQUENCIES

We proceed to compare the observed QPO frequencies from SGRs with the calculated frequencies of torsional oscillations in the bubble phase, together with those of usual torsional oscillations in the crustal region composed of spherical nuclei. We have already discussed the possibility of identifying the observed lowest three QPOs (18, 30, 92.5 Hz) except the 26 Hz QPO in the giant flare of SGR 1806–20 as the $\ell = 2, 3, 10$ fundamental crustal torsional oscillations (Sotani et al. 2013b). In Fig.

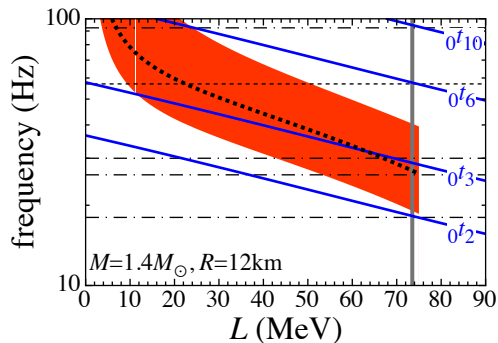


Figure 4. (Color online) Comparison of the observed QPO frequencies in SGR 1806–20 with the crustal torsional oscillations calculated for the stellar model with $M = 1.4M_{\odot}$ and $R = 12$ km. The horizontal lines denote the observed QPO frequencies, where the dot-dash lines correspond to 18, 26, 30, and 92.5 Hz discovered in the giant flare, and the broken line corresponds to 57 Hz found from the shorter and less energetic recurrent 30 bursts. The solid lines represent the calculated $\ell = 2, 3, 6,$ and 10 fundamental frequencies of torsional oscillations in the crustal region composed of spherical nuclei. The vertical solid line denotes the most suitable value of L , 73.5 MeV, for explaining the observed QPOs except 26 Hz in terms of the crustal torsional oscillations. The shaded area denotes the evaluated frequency range of the $\ell = 2$ fundamental oscillation in the bubble phase, which covers the allowed values of the participant ratio \tilde{H}/H . The dotted line is the result for the 50 % participant ratio.

4, we show such an identification in SGR 1806–20 for the stellar models with $M = 1.4M_{\odot}$ and $R = 12$ km. One can find from this figure that the most suitable value of L for explaining the QPOs in terms of the crustal torsional oscillations that have the entrainment effect included by following Chamel (2012) is $L = 73.5$ MeV. We remark that the QPO frequency (57 Hz) discovered from the shorter and less energetic recurrent 30 bursts (Huppenkothen et al. 2014) can also be identified as the $\ell = 6$ fundamental crustal torsional oscillation with the same value of L . With all these successful identifications, there is a problem with explaining the remaining QPO frequency, i.e., 26 Hz, because the interval between 26 and 30 Hz is too small to explain by the fundamental crustal torsional oscillations with neighboring ℓ as long as the lowest QPO is identified as the lowest crustal torsional mode with $\ell = 2$ (Sotani, Kokkotas & Stergioulas 2007). Note that if the lowest QPO is identified as the crustal torsional mode with $\ell = 3$, one can explain all the low-lying QPOs in terms of the crustal torsional modes only when the value of L is assumed to be of order or even larger than 100 MeV (Sotani et al. 2013b; Sotani, Iida & Oyamatsu 2016), being significantly larger than the values deduced from experiments (Tsang et al. 2012).

It is thus interesting to search for the possibility of explaining the 26 Hz QPO in terms of torsional oscillations in the bubble phase in the same stellar model. Recall that these modes can coexist with crustal torsional oscillations in the phase of spherical nuclei, thanks to vanishing shear modulus in the slab phase, and that the $\ell = 2$ fundamental frequency of torsional oscillations in the bubble phase is expected to lie in a range between the frequencies shown in Fig. 3 in the cases of the maximal and minimal enthalpy that contributes to the torsional oscillations. This range corresponds to the shaded region in Fig. 4. Interestingly, 26 Hz is in the middle of this range at the optimal L . In fact, to identify the 26 Hz QPO as the fundamental torsional oscillation in the bubble phase, the participant ratio \tilde{H}/H should be close to 50 %, as can be seen from Fig. 4. Here, the participant ratio is closely related to the entrainment effect; to deduce what portion of nucleons outside bubbles are locked to the motion of the bubbles, we have only to know the participant ratio in the absence of the entrainment effect, which is of order 5–20 %. Note that the L values at which the bubble phase is predicted to occur marginally contain the optimal value of 73.5 MeV. This suggests that neutron stars of $M \geq 1.4M_{\odot}$ and $R \geq 12$ km are favored by the present scenario that requires the presence of bubbles, because the calculated eigenfrequencies and hence the optimal value of L tend to decrease with increasing R and/or M .

To demonstrate that the above scenario works more reasonably for larger and heavier neutron stars, we have repeated the same analysis for the stellar model with $M = 1.8M_{\odot}$ and $R = 14$ km; the results are exhibited in Fig. 5. This figure shows that the same identifications of the observed QPOs work again, while the optimal values of L and \tilde{H}/H are now ~ 54 MeV and ~ 70 %, respectively. We remark in passing that the optimal participant ratio in the bubble phase changes with the stellar model, which may open up the way of constraining the star’s mass and radius once the entrainment effect is known from band calculations.

5 CONCLUSION

In summary, we have examined torsional oscillations in the bubble phase located just above the crust-core boundary of neutron stars. The corresponding eigenfrequencies of the fundamental modes have been calculated for various models of the crust EOS, for various values of the star’s mass and radius, as well as for various values of the participant ratio that reflects

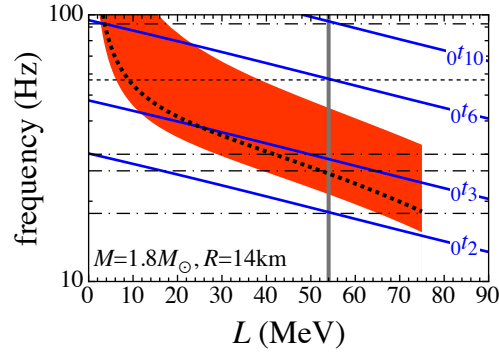


Figure 5. (Color online) Same as Fig. 4 for $M = 1.8M_{\odot}$ and $R = 14$ km. In this case, the dotted line is the result for the 70 % participant ratio.

the entrainment effect, i.e., what portion of nucleons outside the bubbles comove with the oscillating bubbles. The resultant eigenfrequencies in the bubble phase are appreciably higher than the ones in the phase of spherical nuclei. This feature allows one to search for the possibility of reproducing the low-lying QPO frequencies observed from SGRs by appropriately identifying the low-lying QPOs either as a torsional oscillation in the bubble phase or as a usual crustal oscillation in the phase of spherical nuclei, as well as by keeping the value of L reasonable. By simplified calculations, we have succeeded in finding out such a possibility. To make better estimates, however, many questions remain. It would be significant to examine the entrainment effect in the bubble phase based on band calculations (Chamel 2012). For completeness, possible coupling with propagating shear modes in the cylindrical, slab, and cylindrical-hole phases should be allowed for. Magnetic fields, shell and pairing effects on bubbles, electron screening, polycrystalline nature, etc. have been also ignored, but would play a role in modifying the eigenfrequencies in the bubbles phase.

This work was supported in part by Grants-in-Aid for Scientific Research on Innovative Areas through No. 15H00843 and No. 24105008 provided by MEXT and by Grant-in-Aid for Young Scientists (B) through No. 26800133 provided by JSPS.

REFERENCES

- Andersson N., Kokkotas K. D., 1996, *Phys. Rev. Lett.*, 77, 4134
 Chamel N., 2012, *Phys. Rev. C*, 85, 035801
 de Gennes P. G., Prost J., *The Physics of Liquid Crystals*, Oxford Univ. Press, Oxford
 Doneva D. D., Gaertig E., Kokkotas K. D., Krüger C., 2013, *Phys. Rev. D*, 88, 044052
 Gabler M., Cerdá-Durán P., Font J. A., Müller E., Stergioulas N., 2013, *MNRAS*, 430, 1811
 Gearheart M., Newton W. G., Hooker J., Li B. A., 2011, *MNRAS*, 418, 2343
 Hansen C., Cioffi D.F., 1980, *ApJ*, 238, 740
 Haensel P., Potekhin A. Y., Yakovlev D. G., *Neutron Stars 1: Equation of State and Structure*, Springer, New York.
 Huppenkothen D., Heil L. M., Watts A. L., Göğüş E., 2014, *ApJ*, 795, 114
 Hurley K. et al., 1999, *Nature*, 397, L41
 Iida K., Sato K., 1997, *ApJ*, 477, 294
 Israel G. et al., 2005, *ApJ*, 628, L53
 Kobayakov D., Pethick C. J., 2013, *Phys. Rev. C*, 87, 055803
 Kobayakov D., Pethick C. J., 2015, *MNRAS*, 449, L110
 Kouveliotou C. et al., 1998, *Nature*, 393, L235
 Landau L. D., Lifshitz E. M., *Theory of Elasticity 3rd Edition*, Pergamon Press, Oxford
 Lattimer J. M., 1981, *Annu. Rev. Nucl. Part. Sci.*, 31, 337
 Lorenz C. P., Ravenhall D. G., Pethick C. J., 1993, *Phys. Rev. Lett.*, 70, 379
 Ogata S., Ichimaru S., 1990, *Phys. Rev. A*, 42, 4867
 Oyamatsu K., 1993, *Nucl. Phys. A*, 561, 431
 Oyamatsu K., Hashimoto M., Yamada M., 1984, *Prog. Theor. Phys.*, 72, 373
 Oyamatsu K., Iida K., 2003, *Prog. Theor. Phys.*, 109, 631
 Oyamatsu K., Iida K., 2007, *Phys. Rev. C*, 75, 015801
 Passamonti A., Andersson N., 2012, *MNRAS*, 419, 638
 Passamonti A., Pons J. A., 2016, arXiv:1606.02132
 Pethick C. J., Potekhin A. Y., 1998, *Phys. Lett. B*, 427, 7

- Pethick C. J., Ravenhall D. G., 1995, *Annu. Rev. Nucl. Part. Sci.* 45, 429
Samuelsson L., Andersson N., 2007, *MNRAS*, 374, 256
Schumaker B. L., Thorne K. S., 1983, *MNRAS*, 203, 457
Sotani H., Tominaga K., Maeda K. I., 2001, *Phys. Rev. D*, 65, 024010
Sotani H., Kohri K., Harada T., 2004, *Phys. Rev. D*, 69, 084008
Sotani H., Kokkotas K. D., Stergioulas N., 2007, *MNRAS*, 375, 261
Sotani H., 2011, *MNRAS*, 417, L70
Sotani H., Yasutake N., Maruyama T., Tatsumi T., 2011, *Phys. Rev. D*, 83, 024014
Sotani H., Nakazato K., Iida K., Oyamatsu K., 2012, *Phys. Rev. Lett.*, 108, 201101
Sotani H., Nakazato K., Iida K., Oyamatsu K., 2013a, *MNRAS*, 428, L21
Sotani H., Nakazato K., Iida K., Oyamatsu K., 2013b, *MNRAS*, 434, 2060
Sotani H., 2014, *Phys. Lett. B*, 730, 166
Sotani H., Iida K., Oyamatsu K., 2016, *New Astron.*, 43, 80
Sotani H., 2016, *Phys. Rev. D*, 93, 044059
Steiner A. W., Watts A. L., 2009, *Phys. Rev. Lett.*, 103, 181101
Strohmayer T., Van Horn H. M., Ogata S., Iyetomi H., Ichimaru S., 1991, *ApJ.*, 375, 679
Strohmayer T. E., Watts A. L., 2005, *ApJ*, 632, L111
Strohmayer T. E., Watts A. L., 2006, *ApJ*, 653, 593
Tsang M. B. *et al.*, 2012, *Phys. Rev. C*, 86, 015803
Van Horn H. M., Lee U., Epstein, R. I., Collins, T. J. B., in Ichimaru S., Ogata S., eds. *Elementary Processes in Dense Plasmas*, Addison-Wesley, Reading, p. 25
Watanabe G., Iida K., 2003, *Phys. Rev. C*, 68, 045801